

10-19-1992

## Charge Dynamics at the Silicon(001) Surface Studied by Scanning Tunneling Microscopy and Surface Photovoltage

David G. Cahill  
*University of Illinois, Urbana*

R. J. Hamers  
*University of Wisconsin, Madison*

Follow this and additional works at: <https://digitalcommons.usu.edu/microscopy>

 Part of the [Biology Commons](#)

---

### Recommended Citation

Cahill, David G. and Hamers, R. J. (1992) "Charge Dynamics at the Silicon(001) Surface Studied by Scanning Tunneling Microscopy and Surface Photovoltage," *Scanning Microscopy*. Vol. 6 : No. 4 , Article 4. Available at: <https://digitalcommons.usu.edu/microscopy/vol6/iss4/4>

This Article is brought to you for free and open access by the Western Dairy Center at DigitalCommons@USU. It has been accepted for inclusion in Scanning Microscopy by an authorized administrator of DigitalCommons@USU. For more information, please contact [digitalcommons@usu.edu](mailto:digitalcommons@usu.edu).

## CHARGE DYNAMICS AT THE SILICON(001) SURFACE STUDIED BY SCANNING TUNNELING MICROSCOPY AND SURFACE PHOTOVOLTAGE

David G. Cahill\* and R.J. Hamers<sup>1</sup>

Department of Materials Science and Engineering,  
University of Illinois, Urbana, IL 61801

<sup>1</sup>Department of Chemistry, University of Wisconsin, Madison, WI 53706

(Received for publication May 25, 1992 and in revised form October 19, 1992)

### Abstract

Scanning tunneling microscopy measurements of local surface photovoltage of the Si(001) surface reveal the existence of local charging produced by the tunneling current. Since the tunneling current is confined to a region of near atomic dimensions, charge transport between surface and bulk electronic states is probed with high spatial resolution. The surface charge is enhanced while tunneling at the bonded, type-B atomic step and at specific point defects demonstrating atomic-scale variations in the charge dynamics.

### Introduction

With the development of the scanning tunneling microscope (STM), the geometry and electronic structure of surfaces can now be routinely studied with spatial resolution on the scale of single atoms [9, 14]. The goal of the experiments described in this report is to demonstrate an extension of these capabilities to include electronic *transport* properties of the surface.

Our experiments exploit the high current densities inherent to the operation of the STM to create a non-equilibrium charge in the surface electronic states of a Si surface. Charge dynamics can be inferred from these data by realizing that a typical tunneling current of 1 nA corresponds to a tunneling rate of  $6 \times 10^9 \text{ sec}^{-1}$ . For example, if an electron tunneling out of the surface electronic states is replaced on a time scale comparable to  $10^{-10}$  second, the surface will have on average a positive charge. We find this to be the case for the Si(001) surface [3].

To measure the time average of the surface charge produced by the tunneling current, we make use of the surface photovoltage effect [12, 13]. Shining light on the silicon surface generates carriers which act to reduce band-bending produced by surface charges. This reduction in band bending is what we refer to as the surface photovoltage (SPV). When the surface charge is altered locally by the tunneling current, the band bending is changed (see discussion below) and this change in local band bending can be observed through its influence on the SPV.

**Key Words:** Charge dynamics, semiconductor surfaces, photovoltage.

### Experimental Details

The SPV is determined by a double modulation technique [3, 4]: the tunneling current is modulated by periodic illumination from a He-Ne laser and by a sinusoidal modulation  $V_m = 30 \text{ mV rms}$  added to the sample bias. The rms amplitude of the current modulations are measured by separate lockin amplifiers and the two frequencies of modulation are chosen outside the response of the feedback loop that controls the tip-sample separation. The bias induced modulation of the current  $I_m$  measures the differential conductance  $dI/dV = I_m/V_m$ .

\*Address for correspondence:

David G. Cahill,  
Department of Materials Science and Engineering,  
University of Illinois,  
1101 West Springfield Avenue,  
Urbana, IL 61801

Telephone number: (217) 333-6753

FAX number: (217) 244-1631

Since the SPV produces a modulation of the tunneling current  $I_{spv}$  in the same way as a small change in sample bias:

$$I_{spv} = (\pi/\sqrt{2}) \{I(V_{bias} + V_{spv}) - I(V_{bias})\}. \quad (1)$$

The factor  $\pi/\sqrt{2}$  is needed to equate the measured rms  $I_{spv}$  with the peak-to-peak amplitude of the SPV  $V_{spv}$ . We can then determine the SPV from the ratio of the two modulation amplitudes:

$$V_{spv} = (\pi/\sqrt{2}) (I_{spv}/I_m) V_m. \quad (2)$$

For this equation to be exact, the  $I$ - $V$  characteristic would have to be linear (of the form  $I = a + bV$  over the range  $V_{bias} < V < (V_{bias} + V_{spv})$ ). It is straightforward to show however, that the first correction term from any non-linearities is of the order  $d^3I/dV^3$ , see the Appendix. For the bias conditions used in our experiments, this correction term is negligible. The measurement technique has been tested in measurements of the Fermi level position as a function of submonolayer coverages of Ag on Si(111)-7X7 as described in a separate publication [4].

At large laser intensities, we have observed a modulation of the tunneling current produced by thermal expansion of the probe tip. The size of this modulation from 1 mW of laser power at 20 kHz is roughly equivalent to the current modulation produced by a few mV of SPV -- much smaller than the SPV data discussed below.

We perform all experiments at room temperature in ultra-high vacuum (base pressure  $1 \times 10^{-10}$  Torr) using commercial, polished wafers supplied by Wacker Chemitronics (2  $\Omega$ cm B doped). Samples are cleaned with methanol before loading into the UHV chamber and then degassed for 8 hours at 1030 K using resistive heating. Cleaning proceeds by successive flashes to increasingly higher temperatures ending with flashes to 1475 K.

### Results and Discussion

Figure 1 shows the SPV signal as a function of laser power and tunneling current on  $p$  type Si. These data were taken while tunneling at ideal parts of the surface, i.e., avoiding step edges and defects. At small tunneling currents, the SPV approaches the behavior expected for the equilibrium surface charge density and band bending. Increasing the tunneling current at negative sample bias (tunneling of electrons out of the surface states) produces a local, positive charge on the surface electronic states, increases the band bending and enhances the SPV. Complementary behavior is observed on  $n$  type Si: increasing the tunneling current at negative sample bias decreases the band bending and decreases the SPV [3] by roughly the same amount as the SPV is enhanced on  $p$  type Si. The similarity in behavior on  $n$  type Si (forward bias) and  $p$  type Si (reverse bias) argues against an interpretation of our data in terms of metal-insulator-semiconductor transport [2, 21].

Varying the sample bias in the range -2 to 2 volts has a much smaller influence on the measured SPV than the changes produced by varying the tunneling current.

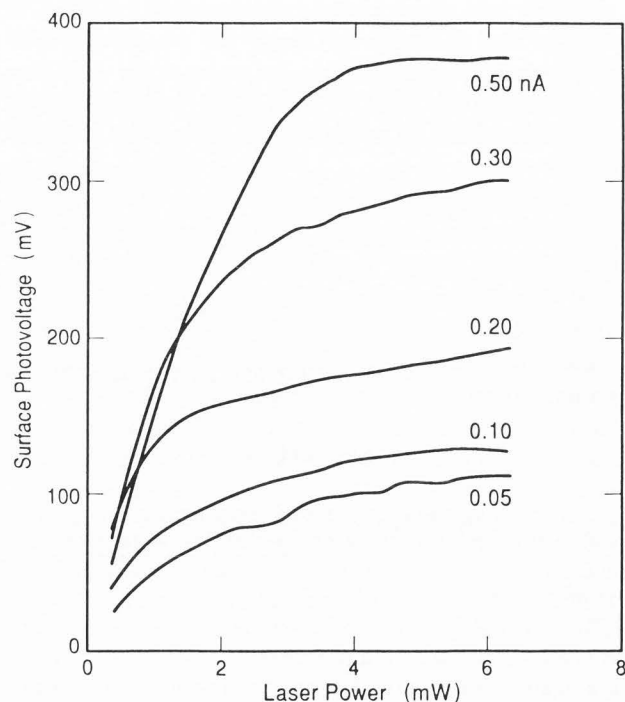


**Figure 1.** Surface photovoltage measured as a function of laser power and tunneling current. Sample is  $p$  type 2  $\Omega$ cm using a sample bias of -1.8 V. Laser is focused to a spot size of 0.3 X 1 mm. Curves are labeled by the average tunneling current in nA.

That the sample bias has little effect on the surface band bending is expected from the high density of electronic states that strongly pin the position of the Fermi level near mid-gap. The influence of the tip-sample electric field on *unpinned* surfaces has been observed in STM  $I$ - $V$  curves [2] and analyzed theoretically [2, 21] in terms of a metal-insulator-semiconductor structure with a negligible density of interface electronic states.

Further support of our assertion that the tunneling current produces a localized surface charge is given by the atomic-scale variations in the SPV data. Figure 2 is an example of data collected by simultaneously measuring the SPV signal while scanning in the usual mode of operation of the STM (constant average current) with a tunneling current large enough to produce significant surface charging. The SPV enhancement is approximately doubled when tunneling within a radius of  $\approx 5$   $\text{\AA}$  surrounding specific defects and step edges (see discussion below) and allow us to rule out bulk spreading resistance or charging of large regions of the surface as explanations for the SPV enhancements shown in Fig. 1. We emphasize that these atomic-scale changes in the SPV are produced by the effects of the tunneling current on the surface. In the limit of small tunneling current, the atomic-scale variations disappear and the SPV is spatially homogeneous [3]. These data are therefore

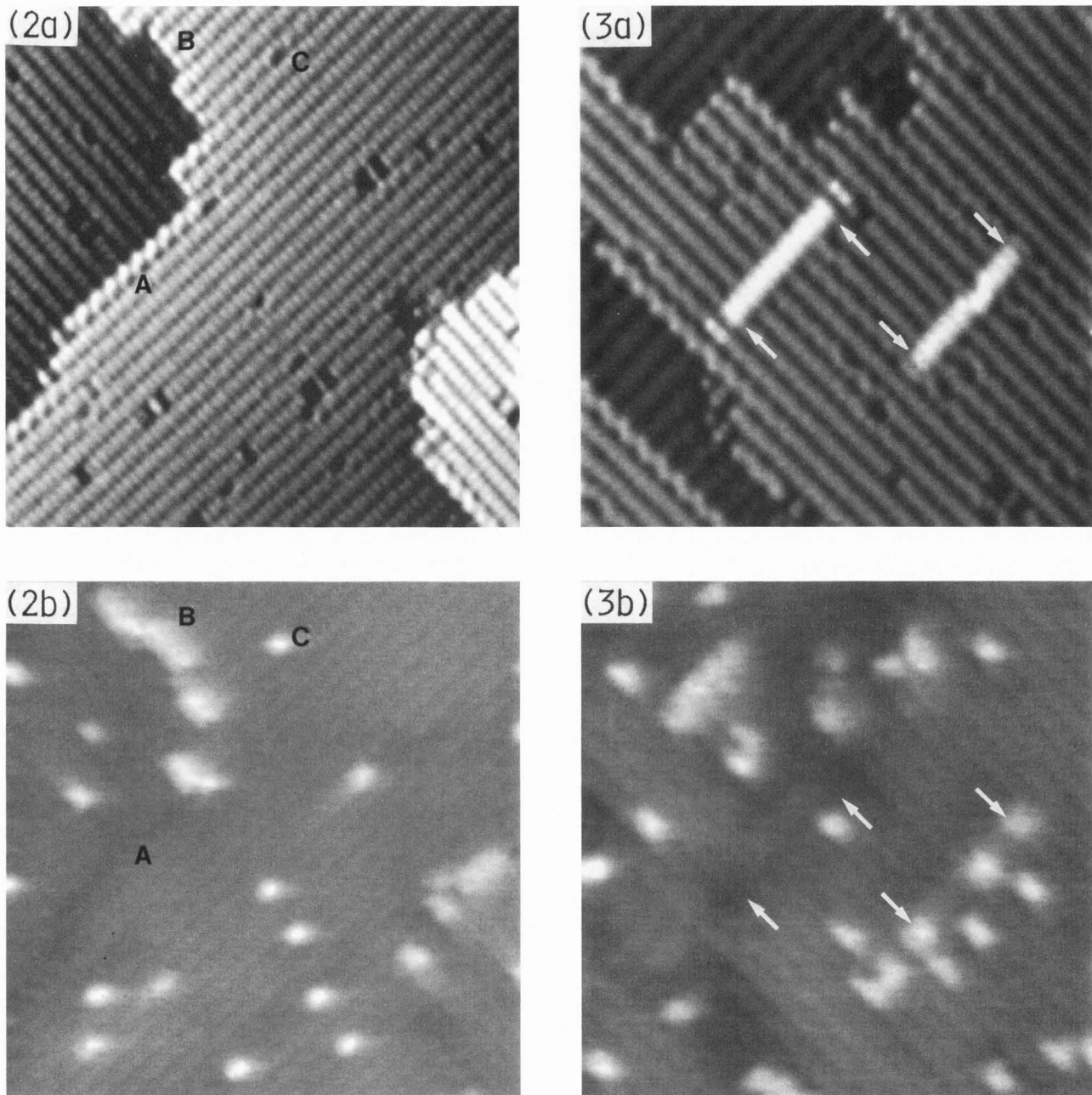


**Figure 2 (at left).** Topography (a) and surface photovoltage (b) at a sample bias of  $-1.8$  V, average tunneling current  $0.4$  nA and laser power  $1.2$  mW focused to a spot size of  $0.3 \times 1$  mm. Scan area is  $200 \times 200$  Å. Type A and B steps and a type C defect are marked with the letters A, B, and C. Black-to-white gray scale in (b) is  $0$ - $300$  mV.

**Figure 3 (at right).** Topography (a) and surface photovoltage (b) of epitaxially grown Si on Si(001) using a sample bias of  $-1.6$  V, average tunneling current  $0.16$  nA, and laser power  $50$   $\mu$ W focused to a spot size of  $0.1 \times 0.3$  mm. Scan area is  $170 \times 170$  Å. Arrows point to the terminations of the two islands discussed in the text. Black-to-white gray scale in (b) is  $0$ - $400$  mV.

fundamentally different than earlier reports of spatial variations in the SPV at defects reported for the Si(111) surface [11, 15].

The data in Fig. 2 also show small but systematic variations ( $\sim 15$  mV) in the SPV measured at the on top and between dimer rows. These variations are an order of magnitude smaller than the changes in SPV at defects and step edges shown in Fig. 2 and may reflect a small systematic error in our measurement technique or may be the result of subtle variations in the surface charge dynamics.

We consistently observe that the surface charge increases at step edges with the dimer rows of the upper terrace running perpendicular to the step edge (type-B step [6]) but never at a step edge with the dimer row of the upper terrace running parallel to the step edge (type-A step). Figure 2 has examples of both types of steps: predominately type-B steps are at upper left and lower right and a predominately type-A step is at the left side of the image. Vacancy defects were previously categorized into two characteristic types [8]: missing dimer defects and the so-called type-C defect, both are visible in Fig. 2. We always observe an increase in the surface charge at type-C defects. Typically, the SPV is unchanged while tunneling at missing dimer defects.

A close inspection of the atomic steps in the lower right corner of Fig. 2 reveals that not all type-B steps produce an increase in the surface charge. Type-B steps have two possible structures depending on the position of the last dimer of the upper terrace relative to the dimer rows of the lower terrace; these two configurations have been referred to as "bonding" (atoms of the lower terrace have dimer bonding) and "non-bonding" (atoms of the lower part of the step do not form dimer bonds) [5]. In agreement with other STM experiments [20] and theoretical calculations [5], we predominately observe type-B steps with the bonding geometry on our clean surfaces; tunneling at this type of step always produces an increase in the surface charge. Tunneling at non-bonding steps does not.

The properties of these step edges are more clearly demonstrated on surfaces prepared by Si epitaxy at low temperatures where we observe both types of type-B step edges with comparable frequency. Approximately 0.1 ML of Si was evaporated by resistive heating of a 3 X 8 mm slice of a *p*-type Si wafer. The Si(001) substrate was held at 300°C during evaporation, a procedure known [10, 17] to produce highly anisotropic islands. At low coverage, these islands are well separated and allow us to study the properties of isolated atomic-scale structures.

Two highly anisotropic islands (each is only one dimer row wide) are shown in Fig. 3 and clearly demonstrate the contrasting properties of the two configurations of the type-B step. Both ends of the island at the left of the image have the non-bonding geometry (the last dimer over the center of the dimer row on the substrate). This structure does not show an increase in surface charge --- in fact, the SPV signal decreases slightly

compared to the ideal surface. (The SPV decreases more strongly at what appears to be an extra dimer that is separated from the island by a gap of one surface lattice constant 3.8 Å. Typically, this structure accompanies islands with non-bonding terminations; similar structures have been observed at anti-phase boundaries on epitaxially grown Si(001) [10]). The contrasting island at lower right of Fig. 3 has both terminations of the bonding type (last dimer in the island lies over a trough between dimers of the substrate). Here the surface charge increases, producing a factor of two increase in the SPV compared to the ideal surface. A type-C defect in the middle of the island at lower right produces a similar increase in the SPV. Since these two islands have roughly the same topography but vastly different SPV behavior, these data demonstrate that the SPV changes cannot be attributed to changes in the geometry of the tip-sample junction.

We now make an estimate of the time averaged magnitude of the surface charge and use the result to estimate the dynamics of charge transfer between the bulk and surface electronic states. Figure 4 depicts schematically our picture of how the SPV responds to a localized surface charge. In the limit of small tunneling current the surface charge is small and the SPV is spatially homogeneous. This behavior has been confirmed in experiments reported previously [3]. At larger tunneling currents the surface charge produced by the tunneling current produces an increase in band bending and the SPV in the vicinity of the probe tip. With the same current while tunneling at a type-C defect or bonding type-B step, the surface charge, band bending and SPV are all enhanced.

We use classical electrostatics to model the band-bending produced by the surface charge. In this model, the surface dimer is replaced by a metal sphere with charge  $Q$  and radius 2 Å (comparable to the volume of a Si dimer) embedded in the surface of a dielectric [16] (for Si  $\epsilon_r = 12$ ). The potential of the sphere (band-bending in a semi-classical model of the Si bulk energy levels) is  $V = -1.1 Q$  volts when  $Q$  is measured in units of the electron charge  $q$ . Figure 1 shows that for large laser intensities the SPV signal saturates at a value of 0.3 V for an average tunneling current of 0.3 nA, 0.2 V larger than the SPV in the limit of small tunneling current, suggesting that the surface charge produces a band-bending of 0.2 V. Using this model, the time averaged surface charge produced by 0.3 nA is  $\approx 0.2q$ .

A time averaged surface charge  $Q = 0.2q$  can be produced by a unit charge existing at the surface 20% of the time. A tunneling current of 0.3 nA corresponds to a tunneling rate of  $2 \times 10^9$  electrons  $\text{sec}^{-1}$ . Our data,  $Q = 0.2q$ , is consistent with a positive charge existing in the surface electronic state for  $10^{-10}$  seconds after an electron tunnels out of the surface, i.e., the decay time of a hole in the surface state is  $\approx 100$  picoseconds. This decay time is comparable to time constants observed in time-resolved photoemission measurements of charge dynamics at the Si(111)-2X1 surface [7].

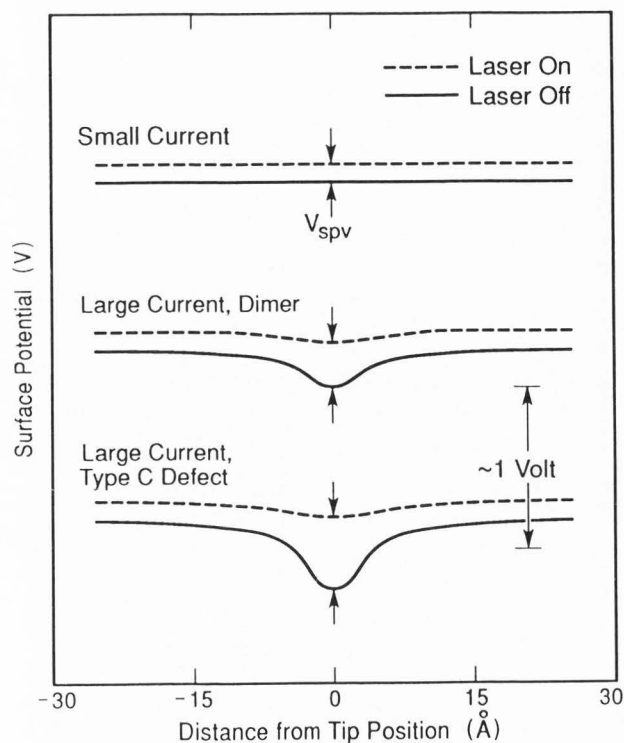


**Figure 4.** Schematic drawing of the influence of a localized charge on the surface photovoltage. **Top:** small tunneling current; **middle:** large tunneling current at the ideal surface; **bottom:** large tunneling current at a type-C defect or bonding configuration of the type-B step.

At type-C defects and the bonding geometry of the type-B step, a factor of two increase in the SPV is observed compared to the ideal surface. These spatial variations can be explained by slower charge dynamics at these sites; if the positive charge exists for twice as long at these sites as it does at ideal parts of the surface, then we expect the size of the surface charge and the SPV signal to increase by a factor of two relative to the ideal surface. The difference in the charge dynamics is probably due to the presence of mid-gap electronic states. Scanning tunneling spectroscopy measurements of the Si(001) surface [1, 8] show that the ideal surface is semiconducting with a surface state band gap of  $\sim 0.6$  V. Using spatially resolved spectroscopy, type-C defects were shown [8], however, to have a significant density of electronic states near the middle of the gap.

To confirm the correlation between mid-gap electronic states and the surface photovoltage enhancements described above, we performed tunneling spectroscopy measurements at the type-B step edge. The differential conductivity  $dI/dV$  was measured with a lock-in amplifier [19]. The tip-sample separation  $s$  was decreased by  $1.5 \text{ \AA}$  as the sample bias approached zero to increase the dynamic range of the measurement. The data have been normalized to constant  $s$  using the experimentally determined function:

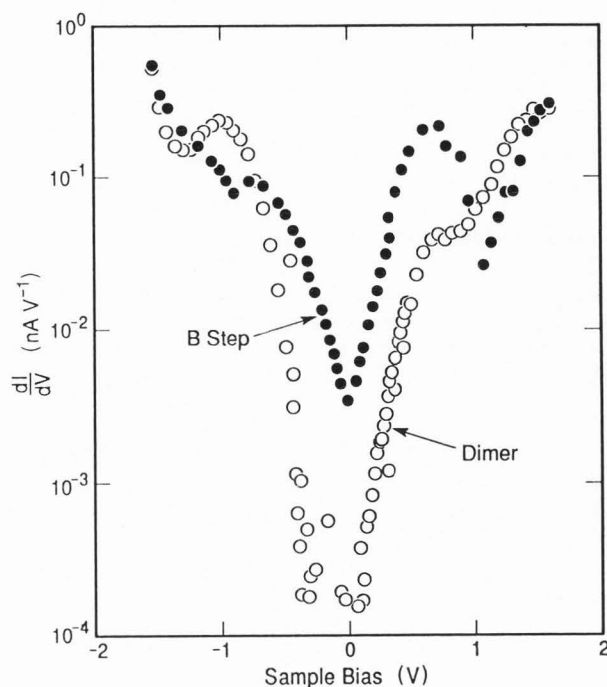


**Figure 5.** Differential conductance measured at an ideal part of the surface (open circles) and at a bonding, type-B step edge (filled circles). The tip-sample separation was stabilized while tunneling at  $-1.6$  V sample bias and  $0.25$  nA tunneling current.

$$I(s) = I(s_0) \exp(1.9(s_0 - s)) \quad (3)$$

when  $s$  is in  $\text{\AA}$ . As is always the case in scanning tunneling spectroscopy, changes in the tip electronic structure can produce variations in the data [18]. The data shown in Fig. 5 were found to be characteristic of the surface and mostly free of artifacts introduced by tip electronic states. The spectroscopy data demonstrate that mid-gap electronic states exist at the bonding, type-B step. We attribute the slower charge dynamics at this site (as in the case of the type-C defect) to the greater separation in energy of these states from the bulk bands but acknowledge that further experimental work (in particular, the temperature dependence of the data) is required.

In conclusion, we have shown that charge dynamics of surface electronic states can be measured by STM. At the Si(001) surface, the tunneling of electrons out of the surface produces a positive charge in the surface electronic states. The decay time of the charged state is on the order of  $10^{-10}$  seconds. This time constant has variations on an atomic scale and is observed to be a factor of 2 slower at the bonding geometry of the type-B step and at type-C surface defects.

#### Acknowledgments

We thank Joe Demuth, Joachim Clabes and Randy Feenstra for helpful discussions on the interpretation of

these experiments. This work was supported in part by the U.S. Office of Naval Research.

### Appendix

For a strictly linear  $I - V$  curve (of the form  $I = a + bV$ ), we showed above that our double modulation technique gives an exact measurement of the surface photovoltage. Here we calculate the size of the correction due to non-linearities of the  $I - V$  characteristic. First, we expand  $I(V)$  around the voltage  $\{(V_b + V_{spv})/2\}$  keeping terms up to order  $(\Delta V)^3$ . We are assuming that the photovoltage signal is a 50% duty cycle square wave.

$$I(V) = I(V_B + V_{SPV}) + \frac{dI}{dV} \Delta V + \frac{1}{2} \frac{d^2 I}{dV^2} (\Delta V)^2 + \frac{1}{6} \frac{d^3 I}{dV^3} (\Delta V)^3$$

$$\Delta V = \frac{V_{SPV}}{2} \frac{4}{\pi} \sum_{(n=1,3,5,\dots)} \frac{1}{n} \sin(n\omega_1 t) + \sqrt{2} V_M \sin(\omega_2 t)$$

$V_b$  is the bias voltage,  $V_{spv}$  is the peak to peak amplitude of the photovoltage signal at frequency  $\omega_1$  and  $V_m$  is the rms amplitude of the modulation applied to the sample bias at frequency  $\omega_2$ . In our experiment, we measure the ratio  $R$  of the output of two lockin amplifier that measure the current modulations at the two modulation frequencies.

$$R = \frac{\int_0^T I(V) \sin(\omega_1 t) dt}{\int_0^T I(V) \sin(\omega_2 t) dt}$$

After some algebra and discarding terms of order  $V_m^2$  we find:

$$R = \frac{\frac{4}{\pi} \frac{dI}{dV} \frac{V_{spv}}{2} + \frac{2}{3\pi} \frac{d^3 I}{dV^3} \left[ \frac{V_{spv}}{2} \right]^3}{\sqrt{2} \frac{dI}{dV} V_m + \frac{\sqrt{2}}{2} \frac{d^3 I}{dV^3} \left[ \frac{V_{spv}}{2} \right]^2 V_m}$$

And finally, treating the terms involving  $d^3 I/dV^3$  as small

$$V_{spv} = \frac{\pi}{\sqrt{2}} R V_m \left[ 1 + \frac{1}{12} \left[ \frac{V_{spv}}{V_{nl}} \right]^2 \right]; \quad V_{nl}^2 = \frac{dI}{dV} \left[ \frac{d^3 I}{dV^3} \right]^{-1}$$

The quantity  $V_{nl}$  is a measure of the non-linearity of the  $I - V$  curve.  $V_{nl}$  can be determined from our tunneling spectroscopy data but its exact value depends on the tip and sample electronic structure and the sample bias. For the relatively large sample biases used in our experiments and for most tips, we find  $V_{nl} \geq 0.4$  volts. At the largest surface photovoltage reported here  $V_{spv} = 0.4$  volts, the correction term is still  $\leq 10\%$ .

### References

- [1] Becker RS, Klitsner T, Vickers JS (1988). Arsenic-terminated silicon and germanium surfaces studied by scanning tunneling microscopy. *J. Microsc.* **152**, 157-165.
- [2] Bell LD, Kaiser WJ, Hecht MH, Grunthaler FJ (1988). Direct control and characterization of a Schottky barrier by scanning tunneling microscopy. *Appl. Phys. Lett.* **52**, 278-280.
- [3] Cahill DG, Hamers RJ (1991). Scanning tunneling microscopy of photoexcited carriers at the Si(001)

surface. *J. Vac. Sci. Technol.* **B 9**, 564-567.

[4] Cahill DG, Hamers RJ (1991). Surface photovoltage of Ag on Si(111)-7X7 by scanning tunneling microscopy. *Phys. Rev.* **B 44**, 1387-1390.

[5] Chadi DJ (1987). Stability of single-layer and bilayer steps on Si(001) surfaces. *Phys. Rev. Lett.* **59**, 1691-1694.

[6] Griffith JE, Kochanski GP (1990). The atomic structure of vicinal Si(001) and Ge(001). *Crit. Rev. Solid State Mat. Sci.* **16**, 255-289.

[7] Halas NJ, Bokor J (1989). Surface recombination on the Si(111)-2X1 surface. *Phys. Rev. Lett.* **62**, 1679-1682.

[8] Hamers RJ, Koehler UK (1989). Determination of the local electronic structure of atomic-sized defects on Si(001) by tunneling spectroscopy. *J. Vac. Sci. Technol.* **A 7**, 2854-2860.

[9] Hamers RJ (1989). Atomic-resolution surface spectroscopy with the scanning tunneling microscope. *Ann. Rev. Phys. Chem.* **40**, 531-559.

[10] Hamers RJ, Koehler UK, Demuth JE (1990). Epitaxial growth of silicon on Si(001) by scanning tunneling microscopy. *J. Vac. Sci. Technol.* **A 8**, 195-200.

[11] Hamers RJ, Markert K (1989). Atomically resolved carrier recombination at Si(111)-7X7 surfaces. *Phys. Rev. Lett.* **64**, 1051-1054.

[12] Hecht MH (1990). Role of photocurrent in low-temperature photoemission studies of Schottky-barrier formation. *Phys. Rev.* **B 41**, 7918-7921.

[13] Hecht MH (1990). Photovoltaic effects in photoemission studies of Schottky barrier formation. *J. Vac. Sci. Technol.* **B 8**, 1018-1021.

[14] Kuk Y, Silverman PJ (1989). Scanning tunneling microscope instrumentation. *Rev. Sci. Instrum.* **60**, 165-180.

[15] Kuk Y, Becker RS, Silverman PJ, Kochanski GP (1990). Optical interactions in the junction of a scanning tunneling microscope. *Phys. Rev. Lett.* **65**, 456-469.

[16] Lorrain P, Corson DR (1970). *Electromagnetic Fields and Waves*. W.H. Freeman, San Francisco, p. 153.

[17] Mo Y-W, Kariotis R, Swartzentruber BS, Webb MB, Lagally MG (1990). Scanning tunneling microscopy study of diffusion, growth, and coarsening of Si on Si(001). *J. Vac. Sci. Technol.* **A 8**, 201-206.

[18] Pelz JP (1991). Tip related artifacts in scanning tunneling spectroscopy. *Phys. Rev.* **B 43**, 6746-6749.

[19] Shih CK, Feenstra RM, Chandrashekar GV (1991). Scanning tunneling microscopy and spectroscopy of BiSrCaCuO 2210 high temperature superconductors. *Phys. Rev.* **B 43**, 7913-7922.

[20] Swartzentruber BS, Mo Y-W, Kariotis R, Lagally MG, Webb MB (1990). Direct determination of step and kink energies on vicinal Si(001). *Phys. Rev. Lett.* **65**, 1913-1916.

[21] Weimer M, Kramer J, Baldeschwieler JD (1989). Band bending and the apparent barrier height in scanning tunneling microscopy. *Phys. Rev.* **B 39**, 5572-5575.

**Editor's Note:** All of the reviewer's concerns were appropriately addressed by text changes, hence there is no Discussion with Reviewers.